Advances in Science and Technology Research Journal

Advances in Science and Technology Research Journal 2024, 18(5), 51–64
https://doi.org/10.12913/22998624/189923
ISSN 2299-8624, License CC-BY 4.0

Received: 2024.05.09
Accepted: 2024.06.26
Published: 2024.08.01

Analysis of the Surface Topography of Fractures Caused by Static and Impact Bending of Polypropylene and Polyamide PA6 Reinforced with Continuous Glass Fibers

Karolina Głowacka[1*], Joanna Małecka[1], Tadeusz Smolnicki[2]

[1] Faculty of Mechanical Engineering, Opole University of Technology, ul. St. Mikołajczyka 5, 45-271 Opole, Poland

[2] Faculty of Mechanical Engineering, Wrocław University of Science and Technology, ul. I. Łukasiewicza 5, Wrocław, Poland

* Corresponding author's e-mail: k.glowacka@po.edu.pl

ABSTRACT

The work analyzes the fracture topography of composite specimens subjected to three-point bending – static and impact. Scanning electron microscopy was used for this purpose. The tests were performed for two different materials, namely polypropylene and polyamide PA6, each reinforced with unidirectional glass fibers. In one case, the fibers were distributed evenly, and in the other, there were areas more and less reinforced with fibers. It was observed that in all cases the tension and compression parts could be clearly distinguished. However, for different materials and with different methods of destruction, varying failure mechanisms were observed, noted based on the analysis of the fracture topography. It was observed that regardless of the loading method and material, in the tensile part there were visibly protruding fibers, and in the compressed part it was the matrix, rather than the fibers, that was destroyed. In the case of statically loaded samples, damage occurred at the macrostructural level, and in the case of dynamically loaded samples, at the microstructural level. Additionally, the samples with uneven fiber distribution were more susceptible to delamination.

Keywords: GFRP, fracture topography, microstructure.

INTRODUCTION

Composite materials are materials consisting of at least two phases. One of these phases acts as a matrix, giving the element its shape, bonding the external fibers, transferring external loads to the reinforcement, and at the same time protecting the fibers against mechanical damage. The second phase is the reinforcing material, most often in the form of fibers, which provide an increase in the strength and stiffness of the material, and sometimes also other properties, depending on the type of reinforcement used [1]. According to the assumptions of composite materials, by combining two phases, the new material is characterized by better properties than each of the component elements, and even better than would result from their mere sum. The appropriate selection of both phases is very important, as adhesive connections between the phases are important to increase strength. The fibers can even influence the crystallization of the matrix [2].

Compared to other materials, such as metals or ceramics, polymers are a better solution in some cases and a worse solution in other. Their structure is more complex, they have lower mechanical strength, lower stiffness, and their heat resistance is lower. They can also be damaged by, for example, ultraviolet light. However, they are cheaper, can be easily processed and are more chemically resistant than other materials. Polymers generally do not conduct heat or electricity, which may be an advantage or disadvantage depending on the situation [3].

Thermosets are mainly used as the matrix of polymer composite materials, especially when

high mechanical strength is required. However, thermoplastic matrix composites have recently become the area of interest of many research groups [4]. This is due to the fact that the commonly used thermoset matrix composites are less ecological and their hardening time is longer than that of thermoplastic matrix composites [5]. Moreover, unlike thermosets, thermoplastics can be repeatedly formed, so they can be recycled [6]. They are also characterized by higher resistance to brittle fracture and greater impact strength. Repeated forming does not change their physical properties, but it should be borne in mind that if the material is exposed to elevated temperatures for too long or subjected to too high temperatures, the properties of the material may deteriorate, especially the resistance to impact loads [3, 7]. The use of composites in a thermoplastic matrix also provides a new spectrum of possibilities for producing elements – it is possible to manufacture products of any shape using additive technology. The use of composites in a thermoplastic matrix can also reduce the costs of manufacturing products. Therefore, they are widely used primarily in the automotive industry and other industries. Their use is limited primarily by lower mechanical strength or brittleness at low temperatures [8].

When it comes to reinforcing plastics, one can distinguish between reinforcing them in the form of fibers (continuous or short) or particles. In particle-reinforced materials, the dispersed phase does not improve the mechanical properties, but gives them new properties, e.g. adding color, increasing the roughness of the manufactured elements, reducing the electrostatic conductivity of the products. Chalk, aluminum oxide, silica or talc are most often used as fillers [9]. The fibers, in turn, improve tensile strength along their length, so the way they are arranged in the structure of the manufactured element is important [10]. The use of short fibers (whiskers) in most cases gives isotropic properties of the obtained product. The possible orientation of the structure may result from the manufacturing technique [11]. The most effective way to improve the strength properties of a material is to reinforce plastics with continuous fibers, which are always arranged in such a way as to provide the element with strength in the directions subjected to the greatest loads [12, 13].

It is often assumed that composite materials in which the reinforcement takes the form of continuous fibers arranged unidirectionally have transversely isotropic properties when the individual layers are also arranged in the same direction [14]. However, opinions in the literature are divided on this issue, especially since in most manufacturing techniques, composites are produced in layers, so air bubbles or voids may appear between them. Even though more and more emphasis is placed on ecology and natural materials are increasingly used to reinforce plastics, such as coconut, bamboo, cotton seeds, flax stalks, pineapple leaves [15], as well as recyclable thermoplastics [16], glass, carbon and aramid fibers are still the leading ones. Glass fibers are most often used in composite everyday objects, primarily due to their relatively low price and processing experience.

The paper compares two materials; in both cases, E-glass fiber (the most popular glass fiber, where 'E' stands for electric) served as the reinforcement, and thermoplastics performed a function of the matrix. Polypropylene acted as the matrix in one material and polyamide PA6 in the other. They are materials often used in industry [17–19], often modified, and therefore widely tested and compared with each other from various angles, i.e. tensile strength, shear, resistance to environmental conditions, as well as microstructural structure [20, 21]. Both polypropylene and polyamide PA6 reinforced with glass fibers are commonly used especially in the automotive industry as well as in electrical and electronical components.

In addition to the mechanical properties of composite materials: their strength, fatigue life, impact strength, crack resistance, etc. [22–25], attention is also paid to their internal structure, especially since it is directly related to the mechanical properties of the material. Manufacturing techniques affect the internal structure of the material, because inclusions, voids, discontinuities, clusters of fibers not filled with the matrix, as well as areas not reinforced with fibers, may already appear at this stage; in addition, the fibers may have an insufficiently good connection with the matrix. Depending on the microstructure of the material, the resistance to both normal and shear stresses increases or decreases. After using particulate fillers, the structure of the matrix may also change, e.g. polyamide PA6 filled with olive pomace powder changes the structure from smooth rectangular pieces to rough with the appearance of craters and cracks all over the surface [26]. Then, under the influence of load or temperature changes, this structure may change and microcracks may form, which deteriorate the strength of the structure

[27]. Depending on the characteristics of the material, a different mechanism of destruction may occur, which may not be noticeable to the unaided eye. Therefore, it is important to analyze the structure of the material both before and after destruction. For this purpose, ultrasonic tests, analyses using microscopes, scanning electron microscopes, computed tomography or numerical tests are carried out [28–30].

A characteristic feature of polyamide PA6 is the strong influence of humidity on its properties [31]. Under the influence of moisture, its stiffness and mechanical strength deteriorate. In the case of fiber-reinforced polyamide, the cracking mechanism of the material changes as well. In the case of dry samples, there is a weaker connection between the matrix and the fibers, which causes the material to become brittle and crack, while in humid samples the failure occurs in the form of pull-out. The literature also contains research results in which polypropylene was combined with an aluminum alloy [32]. It was shown that the interfacial bonding strength increased as a result of anodizing. It was also observed that when the adhesive connection was weak, not only did the mechanical strength of the material deteriorate, but it was visible in the structure of the fracture, which was smooth. On the other hand, when the cohesive connection was weak, the interface was intact and the crack occurred in the structure.

Due to the growing interest in composite materials, especially in the thermoplastic matrix, it is necessary to constantly develop the knowledge about them. It is necessary to acquire not only the knowledge about their strength properties, but also to analyze their method and mechanism of destruction. Thus, it will be possible to use such materials in industry with even greater safety. The work analyzed the fracture topology of statically bent and impact bent samples, using the example of two composites: polyamide PA6 and polypropylene reinforced with continuous glass fibers.

BASIC PROPERTIES OF THE TESTED MATERIALS

As it was explained in the introduction, the article describes a comparison of the fracture topography of two composite materials in which the matrix was a thermoplastic material, while the reinforcement was in the form of continuous fibers arranged unidirectionally. Composites with a thermoset polymer matrix have been used for years; therefore, there are many techniques for producing composites with such a matrix, namely manual lamination, various forms of infusion techniques (e.g. Vacuum Infusion - VI or Resin Transfer Molding - RTM), winding, pultrusion, the use of pre-impregnated layers. To produce composites with a thermoplastic matrix, compression molding or injection molding techniques used are most often. However, the use of these techniques leads to the production of composites with long, but not continuous fibers [33, 34]. Due to the fact that the techniques for producing thermoplastic matrix composites with continuous fibers, although practiced, are not popularly known – unlike in the case of thermoset matrix composites – the paper briefly describes the applied manufacturing method. It is presented graphically in Figures 1–3 [35]. The described manufacturing technique is usually used for fiber-reinforced polymers, but after appropriate surface preparation, it is also possible to produce Fiber Metal Laminates (FMLs) [36, 37]. The composite plates from which the specimens were subsequently

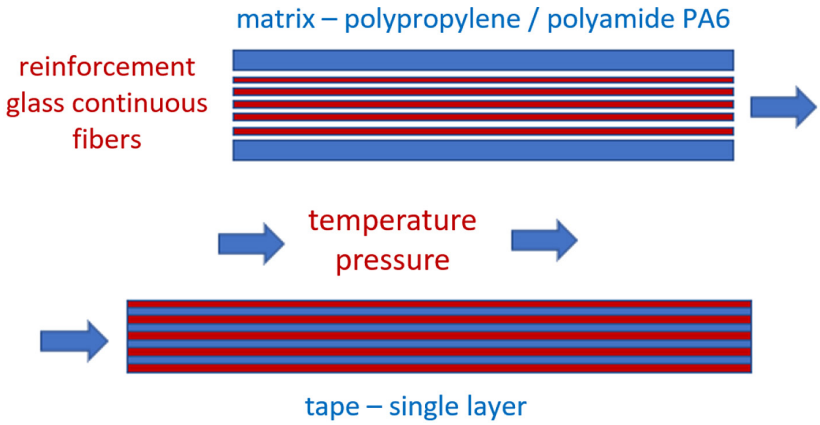

Figure 1. Material manufacturing scheme. Stage 1: producing a single layer

manufactured were manufactured at Chemnitz University of Technology.

In the first stage, single layers were prepared. To obtain them, glass roving was unwound and passed from many bobbins at the same time. These fibers were placed next to each other, resulting in unidirectional reinforcement. In turn, a foil made of thermoplastic material was passed from the top and bottom. Then, under the influence of applied temperature and pressure, a tape was obtained, which was used as the starting material to produce a laminate. The diagram of the first stage is presented in Figure 1.

In the case of a polypropylene composite, tapes with the following basic properties were obtained:

- tape thickness $d = 0.27$ mm,
- percentage of fibers by volume $V_f = 47\%$,

while in the case of a composite made of polyamide PA6, these tapes had the following properties:

- tape thickness $d = 0.30$ mm,
- percentage of fibers by volume $V_f = 39$ %.

Then, the prepared tape was cut into parts of appropriate dimensions. In the next step, the layers were placed one on top of the other, and then, under the influence of temperature and pressure, ready-made plates with the desired layer arrangement were obtained. In the case of the produced specimens, in order to obtain not only unidirectional layers, but entire specimens with unidirectional reinforcement, the fibers in individual layers were arranged in the same direction. The diagram of the second stage is presented in Figure 2.

The course of temperature and pressure over time for composite materials depends on the thermoplastic material used. In the general case, this course is presented in Figure 3. The process consists of three phases: heating, consolidation and then cooling. As shown in the figure, depending on the cooling rate, four variants of courses can be distinguished [38]. In all cases, the maximum temperature at which plasticization will occur, the maximum pressure that will ensure a good connection of the fibers with the matrix, as well as the time of subsequent manufacturing stages should be appropriately selected.

In the case of a polypropylene matrix, preparing the appropriate temperature and pressure characteristics as a function of time is not very hard, as polypropylene is characterized by a wide range of plasticization temperatures. In the literature, one can find both characteristics in which the maximum temperature was 190 °C [39] and those in which the maximum temperature was 230 °C [40]. In the case of polyamide PA6, the temperature range is much narrower. For tested specimens, the process can be described in three steps:

- Step 1: Heating and plasticizing the thermoplastic matrix at a temperature linearly increasing from 25 °C to 220 °C (PP) or 285 °C (PA6), within 10 minutes;
- Step 2: Consolidation of individual fiber-reinforced layers under a pressure of 30 bar, at a constant temperature of 220 °C (PP) or 285 °C (PA6), for 20 minutes;
- Step 3: Cooling and solidification of the obtained multilayer composite by linearly lowering the temperature to room temperature under a constant pressure of 30 bar. Finally, the applied pressure is reduced.

It is worth emphasizing that the quality and strength of composite materials strongly depend on the number of air bubbles and voids occurring between the layers. Bubbles form during

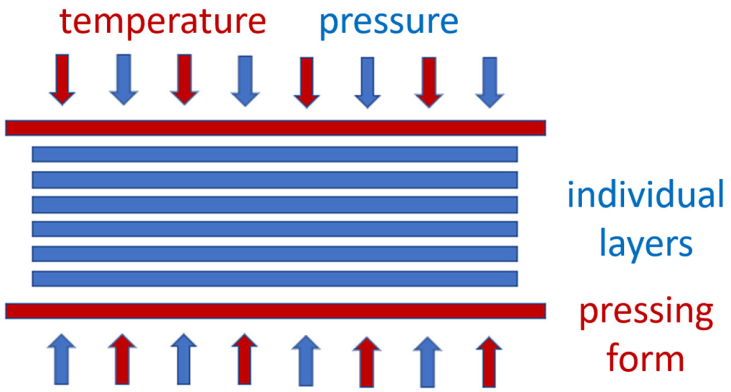

Figure 2. Material manufacturing scheme. Stage 2: producing laminate from separate layers

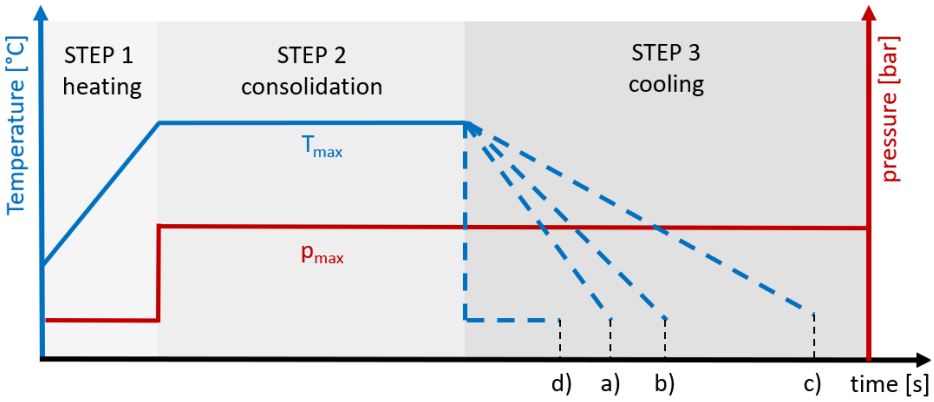

Figure 3. Temperature and pressure during the production of a GFRP laminate with a thermoplastic matrix in variants (a) fast (b) standard (c) slow (d) very fast

consolidation due to the entrapment of air, solvents and moisture. They may accelerate the delamination process [41]. Therefore, an important aspect is the assessment of the quality of the structure after its production, because it will have a significant impact on the strength and method of destruction of the manufactured element.

In the last step, the boards produced according to the described technique were cut into samples with dimensions specified by standards [42, 43]. To avoid introducing additional discontinuities, the water cutting technique was used and the samples were then thoroughly dried. Drying the samples was primarily aimed at avoiding the potential influence of humidity on the properties of polyamide, which was discussed in more detail in the introduction.

Strength tests, both static and impact tests, were carried out in accordance with the ISO standards. In the case of static bending, the dimensions of the tested samples were: 10 mm (height) × 15 mm (width) × 160 mm (length), with span during bending of 120 mm. On the other case, in the case of impact bending the dimensions of the tested samples were: 4 mm (height) × 10 mm (width) × 80 mm (length), with span during bending of 62 mm. In both cases, the loading direction occurred in the direction perpendicular to the length of the sample [44]. The fibers were arranged unidirectionally along the length of the sample.

Table 1 shows the basic properties of these materials. The values for polyamide PA6, polypropylene and glass fibers were taken from the literature; due to the large dispersion in the data, the average value of various literature data was considered. The results for the obtained composite materials were calculated in this paper using mixture theory. As it can be seen, despite the use of a different percentage of fibers due to differences in the stiffness and strength of the component materials, the obtained composites were characterized by comparable mechanical properties. Therefore, it was justified to take these two materials into account.

MICROSTRUCTURE OF THE TESTED MATERIALS

Due to the fact that the microstructure of the material has a significant impact on its strength, the way of its destruction and the topology of fractures, an important step was to conduct a microstructural analysis.

The fracture topography analyses of the cross-section of the tested specimens after the conducted test, were characterized by scanning electron microscopy, using a TESCAN VEGA

Table 1. List of basic properties of the materials

Specification	PA6	PP	GF	PA6 + GF	PP + GF
Density [g/cm^3]	1.14	0.92	2.54	1.69	1.68
Young's modulus [MPa]	2970	1390	73000	30282	35047
Tensile strength [MPa]	75.6	32.2	3500	1411	1662

4 microscope equipped with energy dispersive X-ray spectroscopy (EDS) analyzer. Secondary electrons (SE) were used in the analyses. Conductivity, or the ability of a material to conduct electricity, is an important consideration in SEM sample preparation. In the conducted SEM imaging, analysis samples were coated with a thin layer of conductive material, such as gold.

Scanning electron microscopy (SEM) is widely used in the science of materials and various parameters have been developed to characterize surfaces. The topography of a surface is a direct result of the nature of the material that defines it. Topography is the study and description of the physical features of an area, so the topography of a particular area is its physical shape. In this work, the surface topography of the fracture characteristic zones was analyzed using SEM.

Figures 4 and 5 show the microstructure of the samples with polyamide PA6 and polypropylene matrices, respectively. When analyzing the photographs, voids and bubbles were observed in both materials, which may affect the strength of the manufactured material. However, importantly, no areas between the fibers that were not filled with resin were observed. Due to the similar quality of both manufactured materials, it was considered that they can be compared with each other

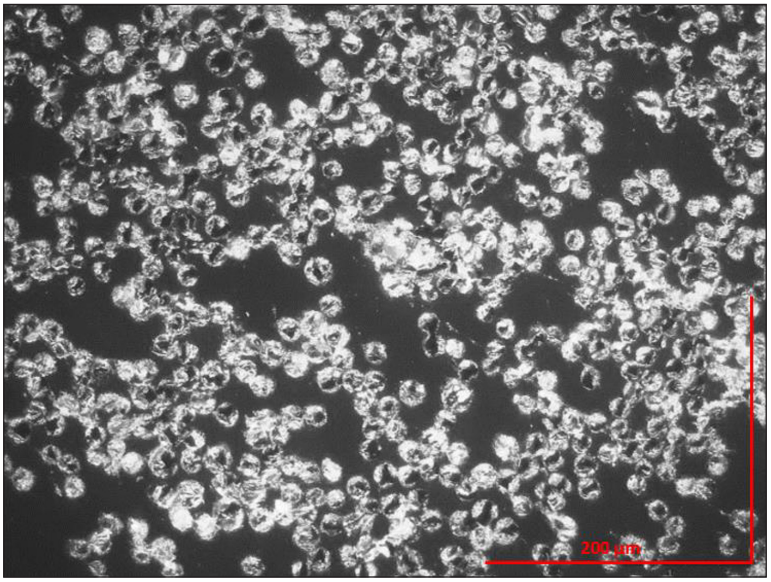

Figure 4. Microstructure of the sample with a polyamide PA6 matrix

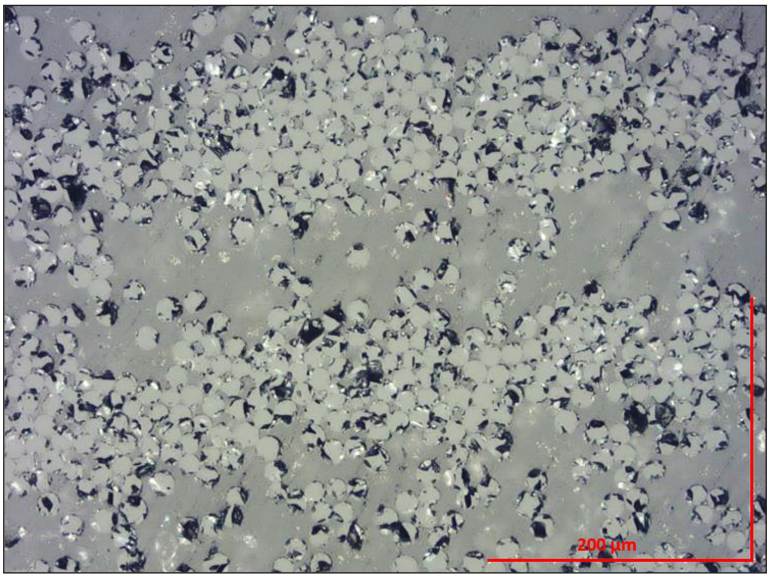

Figure 5. Microstructure of the sample with a polypropylene matrix

for the assessment of fracture topology. While the material in which polyamide PA6 performed a function of the matrix is a material with an even fiber distribution, in the case of the material in which polypropylene performed a function of the matrix, it may be observed that the technique of producing the specimens had a significant impact on their microstructure. There are alternating areas where the percentage of fibers is very high and those where fibers are almost non-existent. This is an understandable phenomenon, resulting from the fact that during the production of a single layer (stage 1 – tape production), there were fibers in the center, while polypropylene, being a matrix, was located at the edges. When force was applied on the press, the polypropylene filled the spaces between the fibers, but the "excess" polypropylene remained on the edges, so the percentage of fibers in these areas is noticeably lower.

Although the unevenness of the fiber filling could be considered a disadvantage, in fact, in the literature [45, 46], and even more in real structures, an uneven material microstructure can be found. Non-uniformity may also appear during operation, for example as a result of temperature changes [47]. Therefore, the analysis and comparison of the fracture topography of even and uneven distribution of fibers will provide a new perspective on the need to consider the non-uniform distribution of fibers in structures.

TOPOGRAPHY OF FRACTURES CAUSED BY BENDING

Whenever a new method of producing materials is tested or in order to understand the properties of a material, not only mechanical strength, but also structural issues are analyzed. This makes it possible to link the structure of a material with its strength, especially since the material properties largely depend on its structure. Therefore, the topography of fractures resulting from three-point, static and impact bending was analyzed.

The first inspection of the fractures of the samples after the strength test showed that in all cases two separate zones were visible. Samples were subjected to bending, in which always part of the material is stretched and part is compressed. As a result, one of the zones corresponds to the compression part, and the other to the tension part. After destruction, the compressed part created a relatively smooth, light-colored structure. In turn, the stretched part was characterized by a dark color after destruction, with protruding fibers.

Figures 6 and 7 show the fracture of samples in a polyamide PA6 matrix (PA6 + GF) bent statically bent and impact bent, respectively. In both cases, there is a fracture across the sample, with the upper part being in compression and the lower part being in tension. It is worth noting here that due to the potentially different stiffness of the material in tension and compression, there is a possibility of shifting the neutral plane. However, based on the fracture analysis of a statically bent sample, such a phenomenon can be excluded. The sizes of the compression and tension parts are comparable, i.e. the neutral plane was located in the middle of the height of the bent samples.

The fracture of the sample in which polypropylene acted as the matrix in the case of static bending was very similar to the fracture of the sample in which the matrix was polyamide PA6. In both cases, there were tension and compression parts. It was possible to distinguish these two areas with the naked eye because in the stretched

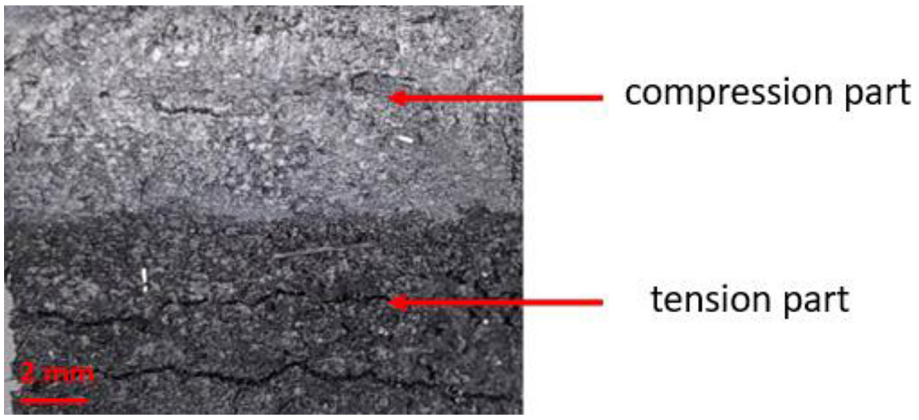

Figure 6. View of the fracture surface of the specimen (PA6 + GF) statically bent

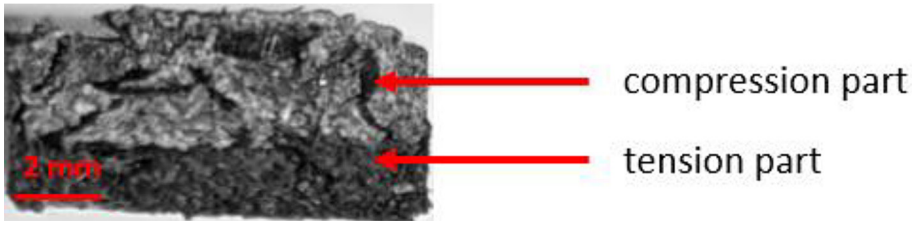

Figure 7. View of the fracture surface of the specimen (PA6 + GF) impact-bent

part, there were protruding fibers in the fracture, as it can be seen in the photo shown in Figure 8.

On the other hand, a large difference occurred in the impact-loaded sample. Although in PP+GF samples there were naturally stretched and compressed areas (just as in PA6 + GF samples), delamination additionally occurred. However, it is not expected that only the material used is important here. What was more important in this case was the uneven distribution of fibers in the loaded material, which is illustrated in Figure 5. The view of the impact-loaded PP + GF sample is shown in Figure 9a. For further analysis, the sample was broken in order to analyze the tensile and compressed parts, as in the case of PA6 + GF samples, not the analysis of the structure from the delamination side – such view is shown in Figure 9b. The first fracture analysis was carried out on the basis of photos of fractures of loaded polyamide PA6 reinforced with glass fibers at 220–300x magnification. They are presented in Figure 10.

The analysis of Figure 10a leads to conclusions mainly regarding the structure of the matrix after applying a static load. Slight porosity was observed, especially in the places with poor adhesive connection between the matrix and the glass fiber surfaces. Separated fragments of the matrix can be observed.

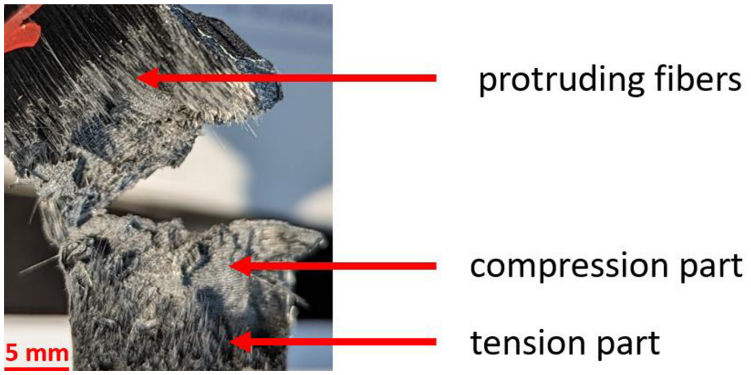

Figure 8. View of the fracture surface of the specimen (PP + GF) statically bent

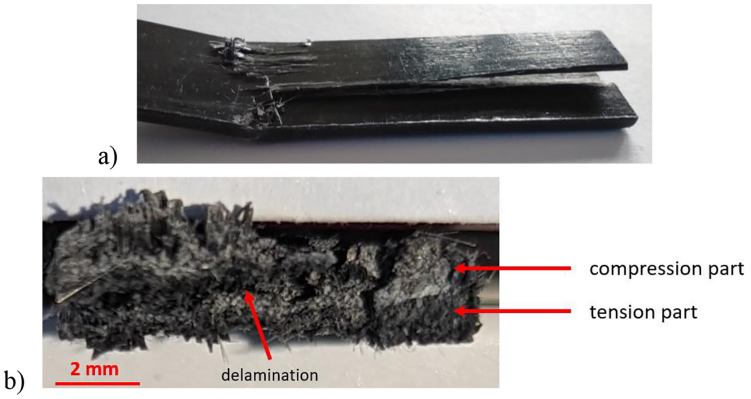

Figure 9. View of the fracture surface of the specimen (PP + GF) impact-bent (a) general view (b) view after additional breaking

In Figure 10b, short protruding glass fibers in the part stretched under static load can be seen much better than with the naked eye. There are also visible protrusions where the fibers were before the break. It was observed that the material did not crack in one plane and clear height differences were visible in the structure.

Figure 10c shows part of the sample which had been in the compression zone during impact-bending. Compared to the compressed part of the statically bent sample, a relatively uniform matrix surface is observed. As it can be seen from the analysis of the figures, the high loading speed caused the failure to occur in one plane, and not at different heights as in the statically loaded sample. When analyzing the microstructure of the sample, it can also be noticed that fragments of the matrix structure are slightly elongated. This is characteristic of polymer materials.

Similarly, to the tensile part, in the case of a statically bent sample, in the case of an impact-bent sample, evenly distributed glass fibers are visible protruding from the material. The holes from which the fibers were also torn out can be seen. Despite the similarity in the structure of statically bent and impact bent samples, clear differences can also be observed. The matrix structure is clearly smoother in the case of the impact-bent

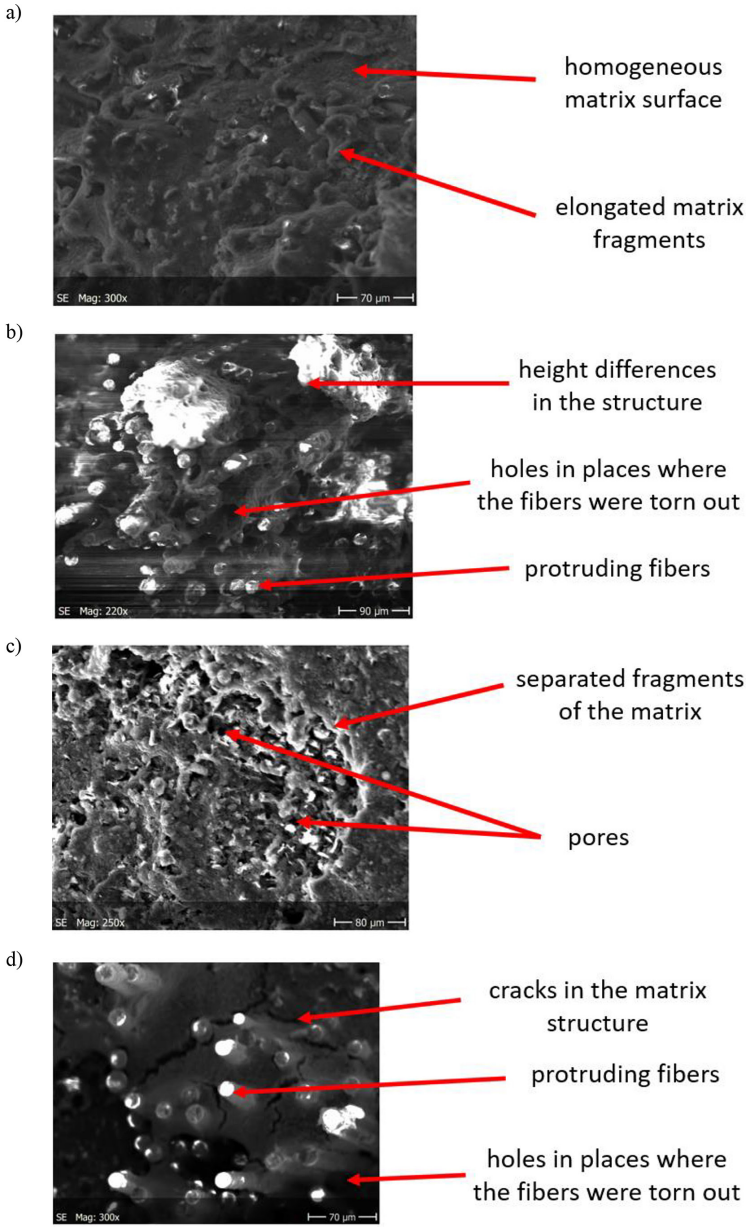

Figure 10. View of the fracture surface of bent specimens (PA6 + GF) at 250–300x magnification (a) static – compression part, (b) static – tension part, (c) impact – compression part, (d) impact – tension part

sample. It can also be observed that the cracking mechanism was different, which resulted in the fact that in the impact-bent sample, visible cracks appeared in the matrix structure.

Different ways of cracking of samples made of composite material (i.e. delamination and fiber tearing) result from different types of stresses arising in the material during bending. Shear stresses lead to sample fracture in form of delamination. In turn, normal stresses arising during bending of the samples lead to fiber rupture.

In impact-bent continuous fiber-reinforced composite samples, similarly to statically bent samples, cracking may occur as a result of two phenomena. Depending on the adhesive shear strength of the material (τ_{adh}), the crack occurs in form of delamination or tearing of the fibers. When the adhesive shear strength is high, fiber rupture occurs, while when the adhesive shear strength is low, delamination occurs. In the examined case, both rupture mechanisms can be observed.

The fracture analysis of the compressed part of the tested materials subjected to static bending shows a clearly elongated structure (Figures 11 and 15) of the material matrix. Large holes around the fibers can be seen; the fibers had room to buckle, which worsens the load transfer of the fibers. Generally compressed composites have much lower strength than tensile ones. In the stretched part of the observed materials (Figures

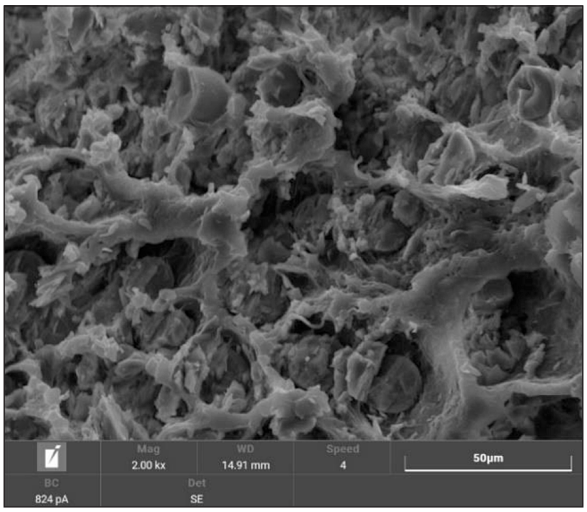

Figure 11. View of the fracture surface of specimen (PA6 + GF) statically bent – compression partv

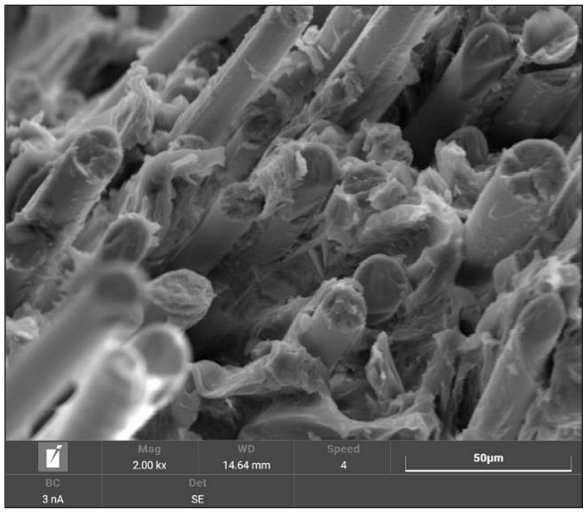

Figure 12. View of the fracture surface of specimen (PA6 + GF) statically bent – tension part

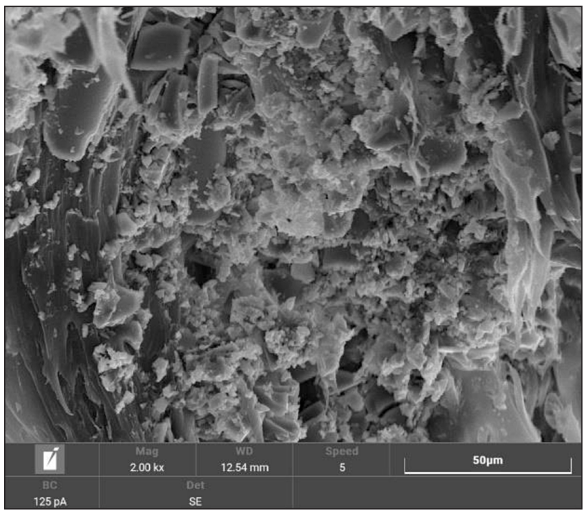

Figure 13. View of the fracture surface of specimen (PA6 + GF) impact bent – compression part

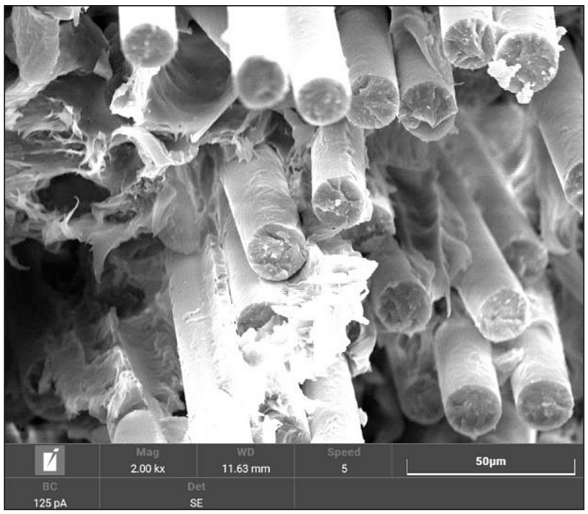

Figure 14. View of the fracture surface of specimen (PA6 + GF) impact bent – tension part

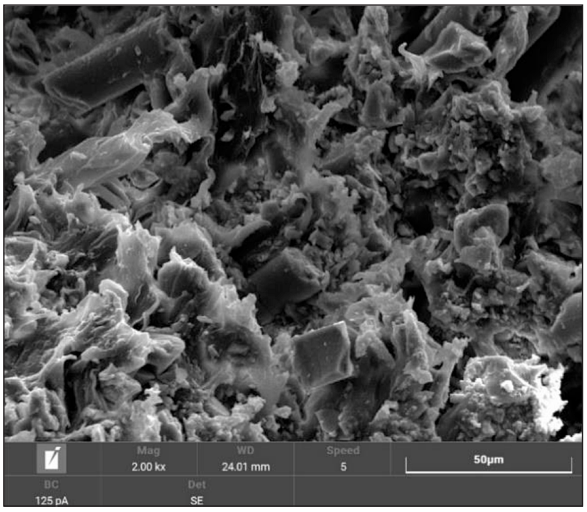

Figure 15. View of the fracture surface of specimen (PP + GF) statically bent – compression part

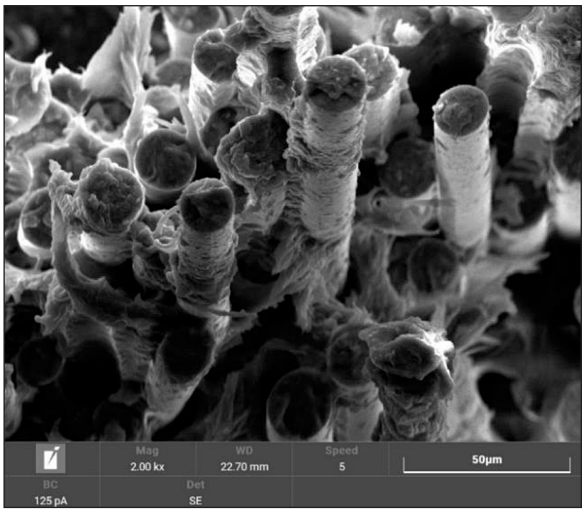

Figure 16. View of the fracture surface of specimen (PP + GF) statically bent – tension part

12 and 16), fibers protruding from the matrix and places from which the fibers were torn out are clearly visible. In the case of the PA6 material (Figure 12), the fibers are evenly connected by the matrix, while in the case of the PP material the fibers are locally arranged very densely, even glued together by the matrix, thus strengthening the entire area, which is related to the obtained test results (the material is "more" durable). At the same time, a change in the fracture height is visible, which probably reflects the place where the fibers were less frequently distributed, which made it easier for the matrix to break.

In the case of impact-bent samples, the fracture analysis of the compressed part shows a much more irregular and brittle structure (Figures 13 and 17). Due to the rapid impact, the material cracked very quickly and the structure did not have time to elongate.

The tensile part of the impact-bent samples is shown in Figures 14 and 18. In the case of the PA6 material, the fibers break in a more brittle manner compared to the statically bent material (Figure 12), moreover, they are torn more from the matrix, and in there is also a crack visible in the matrix itself (Figure 14).

In the case of the PP material, a completely different arrangement of broken fibers can be seen, namely the fibers are also arranged in a perpendicular direction (Figure 18). It can be suspected that due to delamination of the material, some fibers break in a different place than the others and

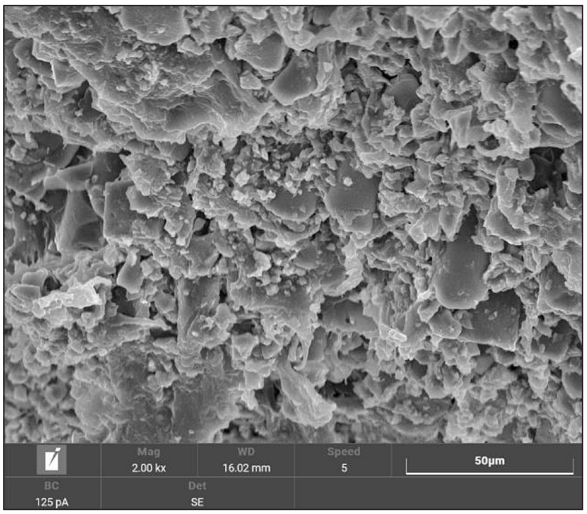

Figure 17. View of the fracture surface of specimen (PP + GF) impact bent – compression part

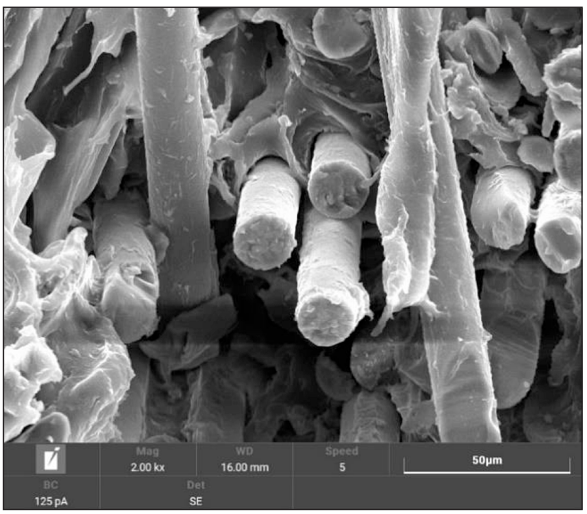

Figure 18. View of the fracture surface of specimen (PP + GF) impact bent – tension part

then bend. Moreover, in this case, cracks at the fiber-matrix interface are also noticeable.

To sum up, in general, in the case of the stretched area, protrusions can be observed resulting from the tearing of glass fibers from the matrix when it bursts, which proves very good adhesion of the matrix to the reinforcing phase. It is worth noting that the reinforcing fibers associated with the matrix remain in approximately equal proportions in both parts of the damaged sample.

CONCLUSIONS

On the basis of the observations of fractures carried out using scanning electron microscopy, a clear influence of the way of loading (static or impact) a specimen made of thermoplastic reinforced with continuous glass fibers arranged unidirectionally on the structure of the material was found. The failure microstructure of bent composite material was analyzed and correlation of the type of load with the material fracture topography was observed. Potentially, after analyzing the fracture of any construction that had failed, it would be possible to identify the reason of the damage, based on analysis conducted in this paper.

It was observed that after the samples were destroyed, it was possible to clearly observe which part of the material was tensed and which was compressed during bending, as well as identify the so-called neutral plane where delamination could occur. In the case of the tensed part, protruding fibers were observed, and using scanning electron microscopy, also the places from which the fibers were torn out during bending. In turn, in the compressed part, destruction of the matrix was observed, for example, pores or separated fragments of the matrix.

The observations revealed the presence of clearly oriented fibers protruding from the material matrix in the tensed part of the material, regardless of the loading method. At the fracture of the impact-loaded samples, in the tensile part, cracks in the matrix are additionally visible, revealing delamination of the material occurring as a result of low adhesive shear strength between the fiber and the matrix. In turn, at the fracture of the statically loaded samples, cracks were visible at the macrostructural level. The crack did not occur in one plane, but characteristic faults were visible.

In the compressed part of the material, regardless of the loading method, the main observation concerned not the fibers, but the matrix. In the case of the samples subjected to the impact test, a relatively uniform surface was observed, while in the case of the samples subjected to the static test, a fragmentarily separated matrix and slight porosity are visible, and the plastic has clearly elongated fragments.

Fracture tests of samples show the degree of material degradation and the reasons for the reduction in functional properties. The photographs of the fractures of samples subjected to compression clearly show the change in the nature of their topography in relation to the samples subjected to tension, regardless of the material used. During the process, destruction of glass fibers is observed, which adversely affects the mechanical properties of the composite materials.

On the basis of the observations, assumptions can be made about a decrease in the strength properties of the material (confirmed by experimental data). Torn fibers may indicate an increased ease of "release" of the reinforcements from the matrix, and the deterioration of adhesion is the result of changes in the structure. This assumption is confirmed by a photo of the fibers, which clearly shows the "growths" of plastic on their surface. The formation of such a structure can be explained by the fact that as a result of the dynamic load during the test, damage to the matrix-matrix structure was much easier than to the matrix-reinforcement structure. In the case of compression, the material is characterized by the presence of numerous composite grooves on the surface, and protruding particles of the material pulled out in the process of mechanical deformation indicate its good adhesion. At the same time, it is visible that they constitute specific discontinuities in the structure, lowering the cross-sectional area that transfers loads. This phenomenon is very dangerous in the case of products that are structurally responsible for the possibility of dangerous damage.

REFERENCES

1. Clyne T.W., Hull D., An Introduction to Composite Materials Third Edition, Cambridge University Press.
2. Zhao S., Cheng L., Guo Y., Zheng Y., Li B. PA6 and Kevlar fiber reinforced isotactic polypropylene: Structure, mechanical properties and crystallization and melting behavior, Materials Design 2012; 35: 749–753.
3. Akca E., Gursel A. A review on the Matrix Toughness of Thermoplastic Materials; Periodicals of

engineering and natural sciences 2015; 3(2): 1–8.

4. Ma Y., Yang Y., Sugahara T., Hamada H. A study on the failure behavior and mechanical properties of unidirectional fiber reinforced thermosetting and thermoplastic composites. Compos Part B: Engineering 2016; 99: 162–72.
5. Tanaka K., Katayama T., Uno K. Eco-efficient manufacturing process for fibre reinforced thermoplastic; High Performance Structures and Materials IV 2008; 97: 203–210.
6. La Mantia F.P., Curto D., Scaffaro R. Recycling of dry and wet polyamide 6; Journal of Applied Polymer Science 2002; 86: 1899–1903.
7. Sinha R. Outlines of Polymer Technology; New Delhi; Prentice-Hall by India Private Limited, 2002.
8. Zhao S.F., Qiu S.C., Zheng Y.Y., Cheng L., Guo Y. Synthesis and characterization of kaolin with polystyrene via in-situ polymerization and their application on polypropylene, Materials & Design 2011, 32(2): 957–963.
9. Cabpbell F.C. Structural Composite Materials; ASM International Materials Park Ohio, 2010.
10. Sinha P.K. Composite materials and Structures; Composite Centre of Excellence AR&DB, Department of Aerospace Engineering 2006.
11. Seong D.G., Kang C., Pak S.Y., Kim C.H., Song Y.S. Influence of fiber length and its distribution in three phase poly(propylene) composites, Compos. B Eng. 2019; 168: 218–225.
12. Thomason J.L. The influence of fibre length and concentration on the properties of glass fibre reinforced polypropylene. 6. The properties of injection moulded long fibre PP at high fibre content. Compos Appl Sci Manuf 2005; 36(7): 995–1003.
13. Visweswaraiah S.B, Selezneva M., Lessard L., Hubert P. Mechanical characterisation and modelling of randomly oriented strand architecture and their hybrids–A general review. J Reinforc Plast Compos 2018; 37(8): 548–80.
14. Kaddour A.S., Hinton M.J. Input data for test cases used in benchmarking triaxial failure theories of composites; Journal of Composite Materials 2012; 46(19–20): 2595–2634.
15. Zimniewska M., Wladyka-Przybylak M., Mankowski J. Cellulosic Bast Fibers, Their Structure and Properties Suitable for Composite Applications; W: Cellulose fibers, bio-, and nano- polymer composites; Springer, Germany 2011; 97–119.
16. Chen X., Ai Y., Wu Q., Cheng S., Wie Y., Potential use of nano calcium carbonate in polypropylene fiber reinforced recycled aggregate concrete: Microstructures and properties evaluation, Construction and Building Materials 2023; 400: 132871.
17. Du B., Li Z., Bai H., Qian L., Zheng C., Liu J., Qiu F., Fan Z., Hu H., Chen L. Mechanical property of long glass fiber reinforced polypropylene composite: from material to car seat frame and bumper beam. Polymers 2022; 14(9): 1814.
18. Cui J., Wang S., Wang S., Li G., Wang P., Liang C. The effects of strain rates on mechanical properties and failure behavior of long glass fiber reinforced thermoplastic composites. Polymers 2019; 11(12).
19. Bondy M., Mohammadkhani P., Magliaro J., Altenhof W. Elevated strain rate characterization of compression molded direct/in-line compounded carbon fibre/polyamide 66 long fibre thermoplastic. Materials 2022; 15(21): 7667.
20. Wang K-H., Chen Y-T., Hwang S-J., Huang C-T., Peng H-S. Influence of back pressure and geometry on microstructure of injection-molded long-glass-fiber-reinforced polypropylene ribbed plates, Polymer Testing 2022; 116: 107797.
21. Güllü A., Ozdemir A., Ozdemir E. Experimental investigation of the effect of glass fibres on ohe mechanical properties of polypropylene (PP) and polyamide 6 (PA6) plastics, Mater. Des. 2006; 27(4): 316–323.
22. Łagoda K., Kurek A., Łagoda T., Błażejewski W., Osiecki T., Kroll L. Cracking of thick-walled fiber composites during bending tests, Theoretical and Applied Fracture Mechanics 2019; 101: 46–52.
23. Vantadori S., Carpinteri A., Głowacka K., Fabrizo G., Osiecki T., Ronchei C., Zanichelli A. Fracture toughness characterisation of a glass fibre-reinforced plastic composite, Fatigue and Fracture of Engineering Materials and Structures 2021; 44(1): 3–13.
24. Głowacka K., Kurek A., Smolnicki T., Łagoda T., Osiecki T., Kroll L. Change in elastic modulus during fatigue bending and torsion of a polymer reinforced with continuous glass fibers, Engineering Failure Analysis 2022; 138: 106341.
25. Głowacka K., Łagoda T. Application of multiaxial fatigue criterion in critical plane to determine lifetime of composite laminates, Engineering Fracture Mechanics, 2023; 292: 109644.
26. Oulidi O., Nakkabi A., ElaraajI., Fahim M., Moualij N. Incorporation of olive pomace as a natural filler in to the PA6 matrix: Effect on the structure and thermal properties of synthetic Polyamide 6, Chemical Engineering Journal Advances 2022; 12: 100399.
27. Gong L., Yu X., Liang Y., Gong X., Du Q. Multiscale deterioration and microstructure of polypropylene fiber concrete by salt freezing, Case Studies in Construction Materials 2023; 18.
28. Zhou W., Mo J., Xiang S., Zeng L. Impact of elevated temperatures on the mechanical properties and microstructure of waste rubber powder modified polypropylene fiber reinforced concrete, Construction and Building Materials 2023; 392: 131982.
29. Sadabadi H., Ghasemi M. Effects of some injection

molding process parameters on fiber orientation tensor of short glass fiber polystyrene composites (SGF/PS), J. Reinforc. Plast. Compos. 2007; (17)26: 1729–1741.

30. Li J., Cao S., Yilmaz E. Analyzing the microstructure of cemented fills adding polypropylene-glass fibers with X-ray micro-computed tomography-Hournal of materials research and technology 2023; 27: 2627–2640.
31. Mohammadkhani P., Magliaro J., Rahimidehgolan F., Khapra T., Altenhof W., Moisture influence on anisotropic mechanical behavior of direct compounded compression molded PA6/Glass LFTs, Composites Part B 2023; 264: 110927.
32. Chen J., Du K., Chen X., Li Y., Huang J., Wu Y., Yang C., Xia X. Influence of surface microstructure on bonding strength of modified polypropylene/aluminum alloy direct adhesion, Applied Surface Science 2019; 489: 392–402.
33. Ning H., Lu N., Hassen A.A., Chawla K., Selim M., Pillay S. A review of long fibre thermoplastic (LFT) composites. Int Mater Rev 2020; 65(3): 164–88.
34. McLeod M., Baril ´E, H´etu J.F., Deaville T., Bureau M.N. Morphological and mechanical comparision of injection and compression moulding in-line compounding of direct long fibre thermoplastics 2010; 1–10.
35. Osiecki T., Gerstenberger C., Hackert A., Timmel T., Kroll L. High-performance fiber reinforced polymer/metal-hybrids for structural lightweight design; Key Engineering Materials 2017; 744: 311–316.
36. Smolnicki M., Duda Sz., Stabla P., Osiecki T. Mechanical investigation on interlaminar behaviour of inverse FML using acoustic emission and finite element method, Composite Structures 2022; 294: 115810.
37. Smolnicki M., Duda Sz., Stabla P., Osiecki T. Mechanical investigation of inverse FML under mode II loading using acoustic emission and finite element method, Composite Structures 2023; 313: 116943.
38. Zopp C., Nestler D., Buschner N., Mende C., Mauersberger S., Troltzsch J., Nendel S., Nendel W., Kroll L., Gehde M. Influence of the cooling behaviour on mechanical properties of carbon fibre-reinforced thermoplastic/metal laminates; Technologies for Lightweight Structures 1(2), Special issue: 3rd International MERGE Technologies Conference 2017; 32–42.
39. Souza B.R., Di Benedetto R.M., Hirayama D., Raponi O., Barbosa C.M., Ancelotti A. C. Jr. Manufacturing and Characterization of Jute/PP Thermoplastic Commingled Composite; Materials Research 2017; 20(2): 458–465.
40. Kabiri A., Liaghat G., Alavi F., Saidpour H., Hedayati S.K., Ansari M., Chizari M. Glass fiber/polypropylene composites with potential of bone fracture fixation plates: manufacturing process and mechanical characterization; Journal of Composite Materials 2020; 54(30): 4903–4919.
41. Bersee H.E.N., Beukers A. Consolidation of thermoplastic composites; Journal of Thermoplastic Composite Materials 2003; 16(5): 433–455.
42. Standard ISO 14125:1998 Fibre-reinforced plastic composites. Determination of flexural properties.
43. Standard ISO 179-1:2010 Plastics. Determination of Charpy impact properties. Part 1: Non-instrumented impact test.
44. Głowacka K. Małecka J. Wpływ statycznej i udarowej próby zginania trójpunktowego na zmiany strukturalne polimerowego kompozytu włóknistego; W: Zmęczenie materiału w eksploatacji maszyn roboczych Część II; Politechnika Opolska; Opole 2020; 17–24 (In Polish).
45. Takahashi K., Yaginuma K., Goto T., Yokozeki T., Okada T, Takahashi T. Electrically conductive carbon fiber reinforced plastics induced by uneven distribution of polyaniline composite micron-sized particles in thermosetting matrix, Composite Science and Technology 2022; 228: 109642.
46. Landis C.M., McMeeking R.M. Stress concentrations in composites with interface sliding, matrix stifness and uneven fiber spacing using shear lag theory, International Journal of Solids and Structures 1999; 36: 4333–4361.
47. Cho C., Choi E.Y., Beom H.G., Kim C.B., Microfrictional dissipation in fiber-reinforced ceramic matrix composites and interfacial shear estimation with a consideration of uneven fiber packing, Journal of Materials Processing Technology 2005; 162–163: 9–14.